Nat. Hazards Earth Syst. Sci. Discuss., https://doi.org/10.5194/nhess-2018-108
Manuscript under review for journal Nat. Hazards Earth Syst. Sci.
Discussion started: 24 April 2018

Natural Hazards and Earth System Sciences
Discussions

Effects of the impact angle on the coefficient of restitution based on a medium-scale laboratory test

Yanhai Wang[1], Wei Jiang[1,2], Shengguo Cheng[2] , Pengcheng Song[2] ,Cong Mao[2]

[1] Hubei Key Laboratory of Disaster Prevention and Mitigation (China Three Gorges University), Yichang, Hubei, 443002, People's Republic of China
[2] Department of Civil, Structural, and Environmental Engineering, University at Buffalo, Buffalo, NY, 14260, United States

Correspondence to: Wei Jiang (jiangweilion@163.com)

Abstract. The reliability of a computer program simulating rockfall trajectory depends on the ascertainment of reasonable values for the coefficients of restitution, which typically vary with the kinematic parameters and terrain conditions. The effects of the impact angle on the coefficients of restitution have been identified and studied using laboratory experiments. However, the laboratory tests performed to date have largely been limited to a small scale. This paper presents the results of a medium-scale laboratory test on the coefficients of restitution for spherical polyhedrons impacting concrete slabs. The specimens were made of natural limestone, and the motion trajectories were recorded by a 3D motion capture system. It is found that only the normal coefficient of restitution R_n and the impact angle α are highly correlated. Comparisons between the results of existing tests and our experiments demonstrate that certain general rules regarding the effect of the impact angle hold regardless of the test scales and conditions. Increasing the impact angle will induce reductions in the values of R_n and the energy coefficient of restitution R_E, whereas it will have a trivial impact on the tangential coefficient of restitution R_t. A small impact angle will likely cause the rebound angle to exceed the impact angle, which typically causes a higher R_n and lower R_E. This phenomenon leads to extreme scatter in the measured data under the conditions of a small impact angle and hinders the prediction of the rockfall trajectory.

1 Introduction

In mountain areas, rockfall is a frequent natural disaster that endangers human lives and infrastructure. Numerous examples of fatalities or infrastructure damage due to rockfall have been reported (Guzzetti, 2003; Pappalardo, 2014). Various protective measures, such as barrier fences, cable nets and rockfall shelters, have been widely used to reduce rockfall hazards. To ensure the efficiency of mitigation techniques, the motion trajectory of the rockfall must be estimated. The trajectory can provide important information, such as the travel distances of possible rockfall events, the bouncing height and kinetic energy level of the rockfall at various positions along the slope.

Determining the rebound behaviour, a succession of rockfalls impacting the slope surface, is the most difficult part of estimating the motion trajectory. Numerous algorithms have been developed to solve this problem, and the progress up to the end of the last century has been summarized by Dorren (2003) and Heidenreich (2004). Due to these efforts, computer

simulation techniques, such as RockFall (Stevens, 1998), Colorado Rockfall Simulation Program (Jones et.al, 2000) and Stone (Guzzetti et.al, 2002), are widely used to acquire motion information for rockfall. The coefficient of restitution is typically used to govern the rebound of a boulder in a computer simulation, which means that the coefficient of restitution must be selected in a reliable manner.

Various techniques, such as laboratory tests (Buzzi et.al, 2012; Asteriou et.al, 2012), field tests (Dorren et.al, 2006; Spadari et al. 2012), back analysis of field evidence (Paronuzzi, 2009) and theoretical estimation (He et.al, 2008), have been used to determine the coefficient of restitution. Variations in the impact conditions, e.g., the material properties of both the blocks and slopes, the shape of the blocks, the roughness of the slope surface and the impact angle, influence the coefficient of restitution considerably. A wide range of artificial and natural materials have been used in tests to determine the effect of the material properties (Wu, 1985; Fornaro et.al, 1990; Robotham et.al, 1995; Chau et.al, 2002), and several correlations between the coefficient of restitution and the Schmidt hammer rebound hardness values (R) have been proposed (Richards et.al, 2001; Asteriou et.al, 2012). Specimens of various shapes, such as spheres, ellipses, discs, cylinders, cubes, pentagons and hexagons, have been considered in laboratory tests to evaluate the effect of block shape (Chau et.al, 1999; Buzzi et.al, 2012), with the results indicating that the normal coefficient of restitution can be sensitive to the block shape in certain cases. Giani et al. (2004) conducted in situ tests on two different slopes, one covered by debris mingled with soil and the other covered by granitic debris, and found that the coefficient of restitution is higher for spherical blocks with smooth surfaces than for blocks with irregular shapes and surfaces. General overviews have been presented for commonly used values of the restitution coefficient (Agliardi and Crosta, 2003; Scioldo, 2006); specifically, the average values and variability ranges of the coefficient of restitution were provided for different terrain classes.

The impact angle, the angle between the directions of the impacting velocity and slope segment, is a kinematic parameter of the falling blocks, indicating only that the terrain conditions involved in estimating the value of the coefficient of restitution may be unreliable. Since Broili (1973) first identified this problem, numerous experiments have been performed to obtain a comprehensive picture of the effects of the impact angle. In situ tests are expensive and not suitable for statistical and parameter analysis; thus, existing studies have largely been performed in the laboratory. The most common method is to capture the trajectory of a block using a high-speed video camera, which is always restrained by the small scale of the laboratory tests. As noted by Heidenreich (2004), the similitude requirements for all parameters involved in the impacting process cannot be easily matched, which creates a barrier to further interpret the results of small-scale laboratory tests.

Hence, the current study employs a 3D motion capture system and special releasing device to perform a medium-scale laboratory experiment. Spherical polyhedrons made of limestone were selected as samples, with a maximum diameter of 20 cm. The landing plate consisted of C25 concrete slabs. To address the effect of the impact angle on the coefficient of restitution, various inclined plate angles and releasing heights were used in free fall tests. Normal and tangential coefficients of restitution as well as the energy coefficient of restitution were calculated and their changing trends in terms of the impact angle were investigated. A comparison between the present study and existing test results has been conducted, and we found that some general laws are irrespective of the test conditions and scales. Under small impact angles, there is a high

Nat. Hazards Earth Syst. Sci. Discuss., https://doi.org/10.5194/nhess-2018-108
Manuscript under review for journal Nat. Hazards Earth Syst. Sci.
Discussion started: 24 April 2018

Natural Hazards and Earth System Sciences
Discussions

possibility of generating a rebound angle larger than the impact angle, which will hinder the evaluation of the influence rule and prediction of the trajectory.

2 Literature review

2.1 Coefficient of restitution

In rockfall analysis, the coefficients of restitution are generally defined as dimensionless values that represent the ratio of velocities or energies of the block before and after it impacts the slope surface. Various definitions of the coefficient of restitution have been suggested in previous studies, but no consensus has been reached on which definition is more appropriate for predicting the rockfall trajectory. As shown in Fig. 1, when one block impacts the slope surface, the impact velocity v_i of the block can be resolved into a normal component v_{ni} and a tangential component v_{ti} according to the slope angle θ. Then, the block leaves with a rebound velocity v_r, which similarly has a normal component v_{nr} and tangential component v_{tr}. The impact angle α and rebound angle β are drawn in Fig. 1.

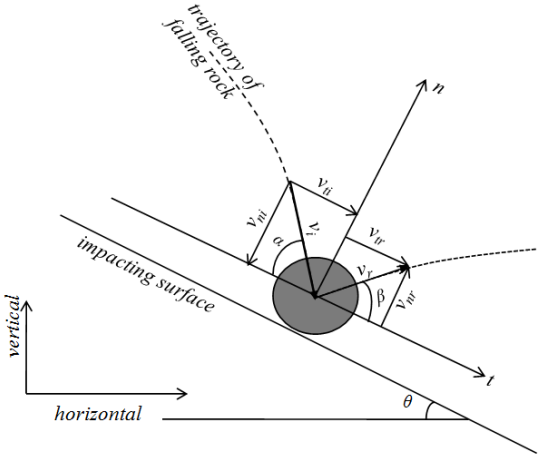

Fig. 1. Resolution of the impact and rebound velocities

The normal and tangential coefficients of restitution are the most commonly used definitions, and these coefficients of restitution are typically denoted as R_n and R_t (or n_{COR} and t_{COR}), respectively. The mathematical expressions of R_n and R_t are

$$R_n = \frac{v_{nr}}{v_{ni}},\ R_t = \frac{v_{tr}}{v_{ti}} \tag{1}$$

These definitions have been adopted and used by many researchers.

Another common definition for the coefficients of restitution, known as R_v (or v_{COR}), is defined as the ratio between the magnitudes of the rebound and impact velocities:

$$R_v = \frac{v_r}{v_i} \tag{2}$$

This definition probably originated from Newton's theory of particle collision and has been used by Habib (1976), Paronuzzi

(1989) and other scholars.

In addition, the ratio of energies before and after impact is used to define the energy coefficient of restitution R_E. When the rotation is neglected and no fragment occurs, the energy coefficient of restitution R_E can be written as

$$R_E = \frac{0.5mv_r^2}{0.5mv_t^2} = \frac{v_r^2}{v_t^2} \quad (3)$$

Here, m represents the mass of the falling block. R_E reflects the energy loss caused by the impact. This definition has been adopted by Bozzolo and Pamini (1986), Azzoni et al. (1995) and Chau et al. (2002).

Of these definitions, R_n and R_t have been most commonly used in rockfall trajectory predictions due to their simplicity in computer simulation software. The existing summaries of the typical values of coefficients of restitution have largely focused on R_n and R_t. In addition to R_n and R_t, the energy coefficient of restitution R_E is calculated to determine the effect of the impact angle on energy dissipation.

1.2 Previous experimental studies on the effects of the impact angle

The impact angle has occasionally been referred to as the slope angle θ (or the impact surface angle) in free-fall tests. However, the impact surface angle is simply another expression because the slope angle θ and impact angle α sum up to 90° under these conditions.

Wu (1985) conducted laboratory tests using rock blocks on a wooden platform and rock slope and suggested that there is a linear correlation between the impact surface angle and the mean value of the restitution coefficient. He proposed that increasing the angle of the impact surface causes the normal coefficient R_n to increase regardless of the block mass and causes the tangential coefficient R_t to decrease slightly.

Richards et al. (2001) executed free-falling tests considering different types of rock and slope conditions and established a correlation between the coefficient of restitution and the Schmidt hammer rebound hardness. The impact surface angle was added to the correlation to reflect its linear improvement effect on the normal coefficient R_n.

Chau et al. (2002) conducted experiments using spherical boulders and a rock slope platform, both made of dental plaster. The free-falling tests indicated that the normal coefficient increases with increases in the impact surface angle, whereas there was no clear correlation with the tangential coefficient.

Cagnoli and Manga (2003) studied oblique collisions of lapilli-size pumice cylinders on flat pumice targets and determined that the variation in the impact angle can influence the rebound angle, the energy loss and the ratios of the velocity components. The normal coefficient decreases as the impact angle approaches 90°.

Asteriou et al. (2012) performed laboratory tests using five types of rocks from Greece. The result of the parabolic drop tests indicated that the kinematic coefficient of restitution R_v was more appropriate than the normal coefficient of restitution for use in correlations with the impact angles. Then, the normal coefficient of restitution could be estimated accounting for the rebound–impact angle ratio.

Buzzi et al. (2012) conducted experiments using flat concrete blocks in four different forms and determined that a

combination of low impact angle, rotational energy and block angularity may result in a normal coefficient of restitution in excess of unity.

These efforts have highlighted the importance of the impact angle with regard to the coefficient of restitution. To date, the knowledge of the coefficient of restitution is still limited with regard to varying impact conditions.

3 Laboratory investigation

3.1 Rock specimens and concrete slabs

All falling rock specimens in this study were natural limestone from the China Three Gouges area and were customized in accordance with the required sizes. As shown in Fig. 2(a), irregular artificial cutting facets constituted the surface of the specimens, and the edges were not smoothed; thus, the shape is called a spherical polyhedron in this study to distinguish it from the standard sphere used in other research studies (Chau, 2002). To address the effect of rock size on the rebound characteristics, two different diameters were considered (D=10 cm and D=20 cm), with corresponding average masses of 1,200 g and 10,000 g. The C25 concrete slabs were produced in a prefabricated concrete factory. As shown in Fig. 2(b), each concrete slab had dimensions of 1,200 mm×500 mm×150 mm. The results obtained using zc3-a type Rebound Hammer indicated that the rebound hardness values (R) of the rock and concrete were 36.0 and 32.5, respectively.

(a) Limestone rocks

(b) Concrete slabs

Fig. 2. Materials used in this study

3.2 Testing apparatus

The apparatus used in this study consisted of a ramp, landing plate and releasing device. The ramp was built by compacting gravelly soil and had an inclined surface with planned angles produced by artificial excavation. Then, two concrete slabs were placed upon the inclined surface to form the landing plate. One device was designed and manufactured specially to catch and release rocks of various sizes. As shown in Fig. 3, the device had four adjustable tongs at the bottom, which could

Nat. Hazards Earth Syst. Sci. Discuss., https://doi.org/10.5194/nhess-2018-108
Manuscript under review for journal Nat. Hazards Earth Syst. Sci.
Discussion started: 24 April 2018

Natural Hazards and Earth System Sciences
Discussions

grasp spherical rocks with diameters from 8 cm to 25 cm. A wireless receiver and electromagnetic relay were installed in the upper portion of the device, offering a wireless method of altering the tong status, grasping or loosing. The device could be connected to an indoor mobile crane by using the top ring, which means that the device could go up and down by managing the crane.

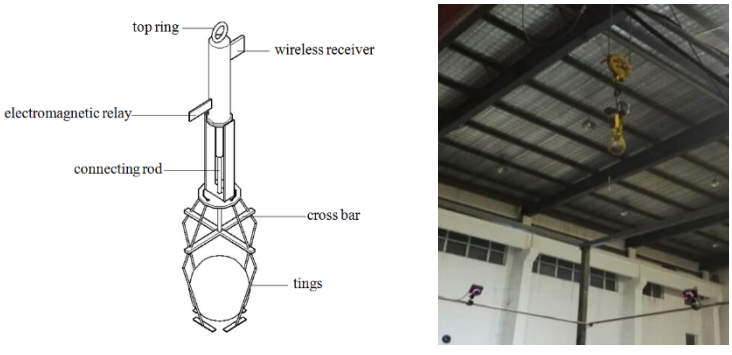

(a) Drafts **(b) Entity**

Fig. 3. Release device

A free-fall test was performed in the experiment, and the complete process of one test is as follows. First, when one spherical polyhedron is prepared to be tested, the tongs are adjusted to accommodate the polyhedron by moving the cross bar up and down. After the block is in the tongs, the grasping state is selected. Then, the device hanging on the indoor crane is moved to the position above the landing plate and lifted to the planned height. Next, by operating the wireless switch, the tongs are loosened, and the block begins to fall. Finally, the block impacts the landing plate, and its motion is recorded. The surface of the concrete slabs becomes worn with successive impacts, as shown in Fig. 4. Once the surface exhibits excessive damage, the used slabs are replaced with new slabs.

(a) Wear on the surface **(b) Slabs to be replaced**

Fig. 4. Damage imposed by impacts

Nat. Hazards Earth Syst. Sci. Discuss., https://doi.org/10.5194/nhess-2018-108
Manuscript under review for journal Nat. Hazards Earth Syst. Sci.
Discussion started: 24 April 2018

Natural Hazards and Earth System Sciences Discussions

3.3 Data acquisition

The spatial motion information of falling rocks was obtained by the Doreal DIMS-9100(8c) Motion Capture System. This system has 8 near-infrared cameras (see Fig. 5 (a)) with an operating speed of 60 fps and can capture the spatial trails of markers attached to the surface of the block, as shown in Fig. 5(b). Then, the motion analysis program provides the spatial motion information of the centre of the falling rocks, e.g., their positions, velocities and accelerations. Finally, the coefficient of restitution can be calculated according to Eqs. (1)-(3) for subsequent analysis.

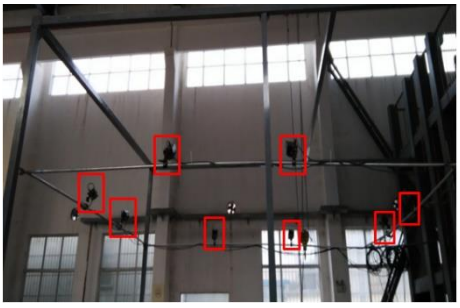

(a) Distribution of 8 infrared cameras

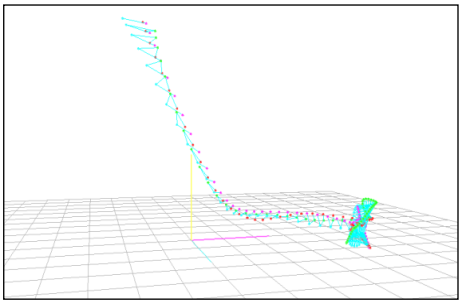

(b) Trails of marked points in one test

Fig. 5. Motion capture instruments

3.4 Experimental program

Four different inclined angles θ of the landing plate (30°, 45°, 60° and 75°) were considered in this study to determine the effect of the impact angle on the COR. Under free-fall test conditions, the impact angles are approximately related to the incline angle θ of the landing plate. Rock specimens were released at three different heights of 2.5 m, 3.5 m and 4.5 m upon the inclined concrete slabs. The impact velocities varied from 6.7 to 9.3 m/s.

However, two experiments do not necessarily have identical release conditions even if they have the same release height and use the same specimen because the positions on which the tongs catch the specimen may differ slightly in any two tests. In Table 1, the initial conditions of our experiment are presented, in addition to the resulting impact velocities and angles, R_n, R_t, R_E and the rebound angles.

Table 1. Initial conditions and results of our experiments

Size (cm)	Inclined Angle θ (°)	Release Height (m)	Impact Velocities (m/s)		Impact Angles α (°)		R_n		R_t		R_E		Rebound Angles β (°)		Test Numbers N
			Mean	Std Dev	Mean	Std Dev	Mean	Std Dev	Mean	Std Dev	Mean	Std Dev	Mean	Std Dev	
10	*30*	*2.5*	*6.50*	*0.11*	*57.25*	*1.41*	*0.42*	*0.09*	*0.80*	*0.03*	*0.32*	*0.05*	*38.31*	*6.21*	*4*
		3.5	*7.75*	*0.06*	*57.21*	*1.44*	*0.38*	*0.04*	*0.92*	*0.08*	*0.35*	*0.04*	*32.88*	*3.94*	*3*
		4.5	*9.06*	*0.16*	*58.27*	*1.33*	*0.39*	*0.03*	*0.88*	*0.04*	*0.32*	*0.01*	*35.49*	*3.23*	*3*

		2.5	6.41	0.17	39.42	1.24	0.53	0.04	0.82	0.09	0.52	0.08	28.47	3.52	4
	45	3.5	7.72	0.09	39.07	0.66	0.52	0.02	0.78	0.08	0.47	0.08	28.48	2.85	3
		4.5	8.76	0.10	39.77	0.20	0.58	0.07	0.82	0.06	0.54	0.07	30.47	3.76	3
		2.5	6.51	0.21	25.06	1.21	0.76	0.06	0.69	0.03	0.49	0.04	27.17	1.77	3
	60	3.5	7.94	0.16	25.76	0.91	0.88	0.11	0.70	0.12	0.56	0.12	32.13	8.13	3
		4.5	8.80	0.17	26.99	1.62	0.53	0.17	0.70	0.02	0.45	0.02	20.92	5.70	3
		2.5	6.47	0.16	12.79	1.71	1.00	0.11	0.53	0.03	0.31	0.03	23.35	3.16	3
	75	3.5	7.91	0.08	10.06	0.73	1.11	0.27	0.65	0.19	0.48	0.25	18.65	7.38	3
		4.5	9.12	0.20	9.76	1.21	1.68	0.30	0.49	0.08	0.33	0.05	31.24	9.73	3
		2.5	6.47	0.20	57.69	0.75	0.40	0.01	0.87	0.03	0.33	0.02	35.77	1.49	3
	30	3.5	7.80	0.11	58.09	1.44	0.31	0.03	0.89	0.11	0.29	0.03	29.41	4.18	3
		4.5	8.89	0.19	58.02	1.63	0.37	0.03	0.85	0.05	0.30	0.04	34.90	3.15	4
		2.5	6.47	0.21	40.97	3.14	0.56	0.03	0.73	0.02	0.44	0.03	33.89	4.48	3
	45	3.5	7.96	0.05	40.05	1.55	0.49	0.05	0.70	0.04	0.39	0.05	30.54	3.03	3
		4.5	8.74	0.13	40.16	0.22	0.47	0.09	0.86	0.04	0.52	0.06	24.68	3.77	3
20		2.5	6.33	0.05	26.76	2.40	0.76	0.08	0.72	0.02	0.53	0.04	28.15	2.71	3
	60	3.5	7.57	0.09	24.96	0.38	0.74	0.13	0.66	0.07	0.46	0.07	27.64	5.60	3
		4.5	8.76	0.19	27.44	1.57	0.64	0.12	0.63	0.10	0.41	0.09	28.29	6.11	3
		2.5	6.08	0.16	11.39	1.52	0.79	0.07	0.67	0.13	0.48	0.17	14.32	5.67	3
	75	3.5	7.30	0.29	11.56	2.05	1.08	0.21	0.64	0.16	0.46	0.19	19.58	5.83	3
		4.5	7.97	0.26	10.63	2.90	1.17	0.18	0.62	0.16	0.44	0.20	19.41	3.23	3

4 Analysis of the results

Although the mean values and standard deviations have been calculated for the release conditions and corresponding results, data points are considered in this section to provide a broad perspective for an evaluation of the effect of the impact angle.

4.1 Effect of the impact angle on R_n and R_t

The four different inclined angles of the landing plate (θ=30°, 45°, 60° and 75°) induce four intervals of impact angles, 55°<α<60°, 36°<α<44°, 23°<α<30° and 6°<α<15°. The effect of impact angle on the normal coefficient of restitution R_n is shown in Fig. 6. When the impact angle is smaller than 15°, the values of R_n range from 0.709 to 1.989, and more than 60% of the values of R_n are larger than 1.0. A larger impact angle tends to produce a smaller value of R_n and reduce the discreteness. The values of R_n range from 0.372 to 1.034 in (23°, 30°), from 0.336 to 0.653 in (36°, 44°), and from 0.277 to 0.519 in (55°°, 60°).

Nat. Hazards Earth Syst. Sci. Discuss., https://doi.org/10.5194/nhess-2018-108
Manuscript under review for journal Nat. Hazards Earth Syst. Sci.
Discussion started: 24 April 2018

Data points were matched for two different specimen sizes using different types of functions, and the comparison indicated that the power function has the maximum value of the correlation coefficient R^2. The correlation of R_n and the impact angle α can be expressed as

D=20 cm: $R_n = 4.4123\alpha^{-0.599}, R^2 = 0.8106$ (4-1)

D=10 cm: $R_n = 5.9972\alpha^{-0.666}, R^2 = 0.7905$ (4-2)

The trend for specimens with size D=20 cm is plotted as a solid line in Fig. 6, whereas the line is dashed for size D=10 cm. The dashed line is above the solid line initially, although the gap narrows with increases in the impact angle. When the impact angle is larger than 30°, these two lines do not exhibit a clear difference. Therefore, small specimens are more likely to have a high R_n than large specimens with small impact angles, and the effect of the rock size on R_n can be neglected when the impact angle is more than 30°.

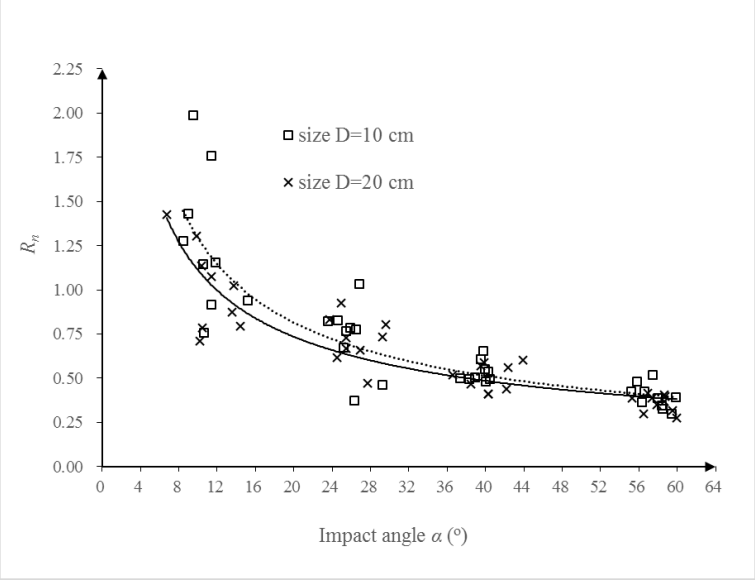

Fig. 6. Effect of the impact angle on R_n

The impact angle has a different effect on the tangential coefficient of restitution R_t than on R_n. As shown in Fig. 7, R_t increases slightly with increases in the impact angle, whereas R_t decreases slightly. The values of R_t range from 0.426 to 0.909 in (6°, 15°), from 0.495 to 0.856 in (23°, 30°), from 0.653 to 0.958 in (36°, 44°), and from 0.796 to 1.038 in (55°, 60°). Various types of functions are adopted to fit data points, as no one function can provide a correlation coefficient R^2 of more than 0.60. Considering that Wu (1985) suggested a linear relationship between R_t and the impact angle α, a linear function is employed to reflect the correlation:

D=20 cm: $R_t = 0.0049\alpha + 0.5679, R^2 = 0.4247$ (5-1)

D=10 cm: $R_t = 0.0066\alpha + 0.5096, R^2 = 0.5703$ (5-2)

In Fig. 7, the solid line represents the trend for specimens with D=20 cm, and the dashed line represents the trend for D=10 cm. No distinct difference can be distinguished between the two lines.

Nat. Hazards Earth Syst. Sci. Discuss., https://doi.org/10.5194/nhess-2018-108
Manuscript under review for journal Nat. Hazards Earth Syst. Sci.
Discussion started: 24 April 2018

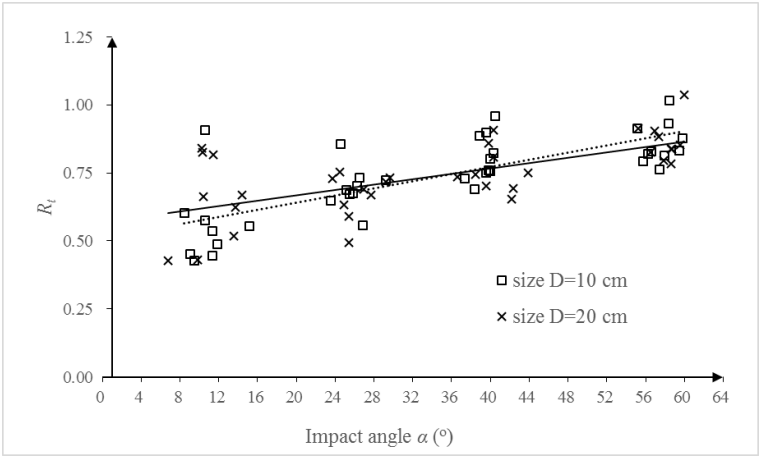

Fig. 7. Effect of the impact angle on R_t

4.2 Effect of the impact angle on R_E

Based on Eq. (3), the effect of the impact angle on the coefficient of energy restitution R_E is illustrated in Fig. 8. The values of R_E range from 0.208 to 0.818 in (6°, 15°), from 0.297 to 0.724 in (23°, 30°), from 0.322 to 0.634 in (36°, 44°), and from 0.261 to 0.391 in (55°, 60°). As the impact angle increases, the peak values of R_E of the four impact angle intervals decrease, and R_E values become increasingly concentrated. However, the mean value of R_E has a more complex changing trend. In Fig. 8, the mean value of R_E in the first impact angle interval is slightly smaller than that in the second impact angle interval. The second impact angle interval has the same approximate average R_E as the third impact angle interval. From the third to the fourth impact angle intervals, there is a remarkable reduction in R_E values. The smaller impact angles induce less energy loss than larger impact angles (Chau 2002; Asteriou 2012). However, the relationship between energy losses with impact angles may not be suitable for small impact angles. By comparison, a polynomial function is applied to match data points, and its correlation coefficient R^2 is smaller than 0.40.

D=20 cm: $R_E = -0.0002a^2 + 0.0077a + 0.3875, R^2 = 0.2894$ (6-1)

D=10 cm: $R_t = -0.0003a^2 + 0.0194a + 0.2011, R^2 = 0.3789$ (6-2)

In Fig. 8, the solid line denotes the results for D=20 cm, and the dashed line denotes the results for D=10 cm. When the impact angle is greater than 23°, the dashed line is slightly above the solid line, which indicates that the smaller specimens typically have less energy loss than the larger specimens. Moreover, in all four impact angle intervals, the maximum R_E values occur for D=10 cm.

Nat. Hazards Earth Syst. Sci. Discuss., https://doi.org/10.5194/nhess-2018-108
Manuscript under review for journal Nat. Hazards Earth Syst. Sci.
Discussion started: 24 April 2018

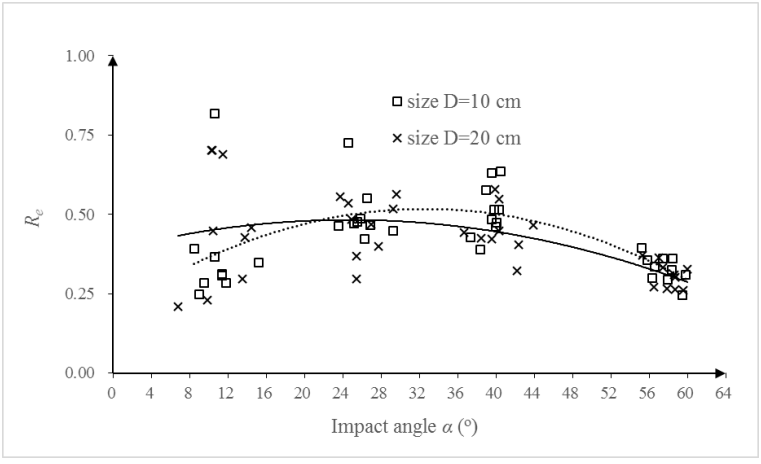

Fig. 8. Effect of the impact angle on R_E

4.3 Relationship between the impact angle and rebound angle

Although there are certain differences between the results for the different-sized specimens, the effect of rock size on the coefficient of restitution is negligible compared with the effect of the impact angle. Hence, no differentiation is made between the data for D=20 cm or from D=10 cm in this section.

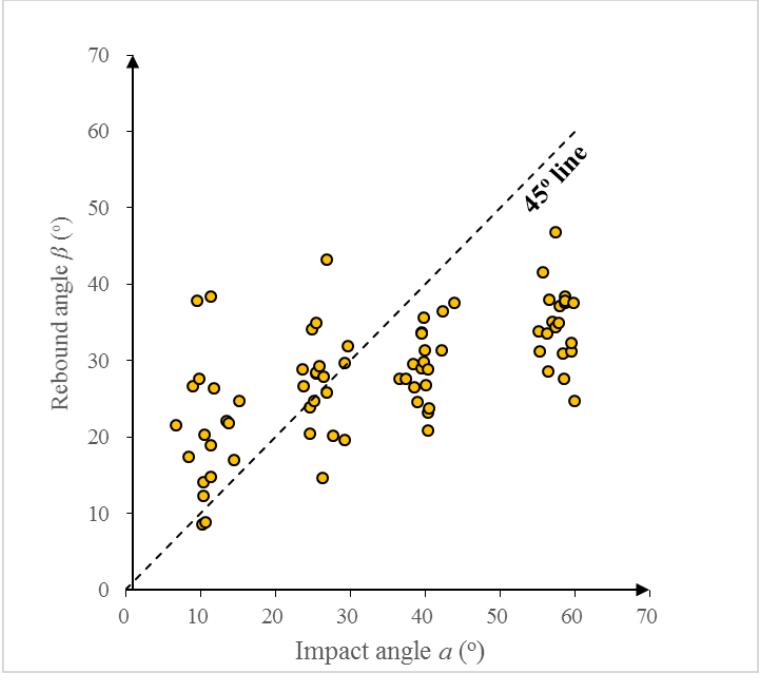

Fig. 9. Rebound angle versus impact angle

The relationship between the impact angle and the rebound angle based on the test results is shown in Fig. 9. Assuming that the falling rock is spherical and that no energy dissipation occurs during the collision, the rebound angle should theoretically

Nat. Hazards Earth Syst. Sci. Discuss., https://doi.org/10.5194/nhess-2018-108
Manuscript under review for journal Nat. Hazards Earth Syst. Sci.
Discussion started: 24 April 2018

be equal to the impact angle, which would result in the data points lying on the 45° line in Fig. 9. However, the test results are almost entirely located above the 45° line in the first impact angle interval, and nearly 50% of the test results are above the line in the second interval. The data points are stably located below the 45° line until the impact angle increases to 36°. A rebound angle greater than the impact angle does not violate the energy dissipation rule. The experimental results presented in Section 4.2 demonstrated that the energy loss constituted 50-75% of the total energy for many data points in the first impact angle interval. Therefore, the energy loss level cannot be assessed by comparing the rebound and impact angle directly.

This phenomenon only implies that the rebound motion probably has an unexpected direction. Fig. 10 plots the velocity direction transition caused by the impact, in which diagrams are individually drawn for four impact angle intervals. For a uniform expression, the landing plate is denoted as the bottom black line. Although the impact velocity directions are concentrated for each impact angle interval, the rebound velocity directions vary considerably. The variation for the interval (36°, 44°) is the smallest of all intervals.

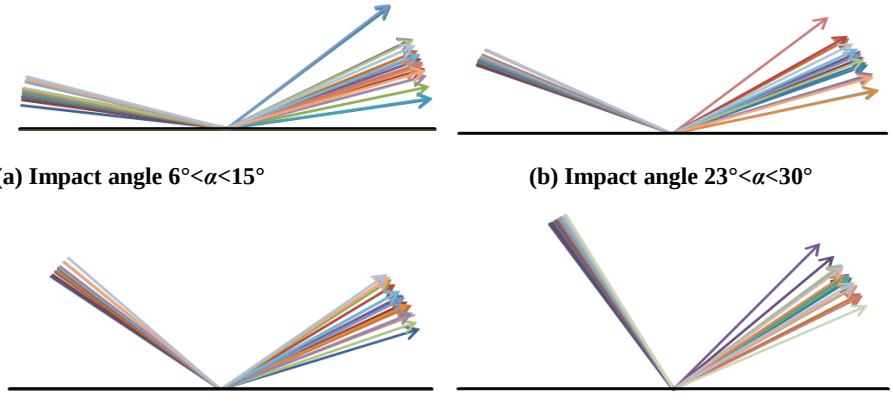

(a) Impact angle 6°<α<15° **(b) Impact angle 23°<α<30°**

(c) Impact angle 36°<α<44° **(d) Impact angle 55°<α<60°**

Fig. 10. Diagram of the velocity direction transitions

In summary, our experimental results demonstrate that as the impact angle α increases, the normal coefficient of restitution R_n will decrease and the tangential coefficient of restitution R_t will increase slightly. The relationship between the impact angle α and energy coefficient R_E is complex; thus, a definitive conclusion cannot be drawn here. The mathematical fitting results demonstrate that only R_n and the impact angle α are significantly correlated.

5 Comparison with existing studies

Over the last few decades, to achieve control over specific critical parameters, laboratory tests have been performed to determine the effect of the impact angle on the coefficient of restitution and other motion parameters (Chau 2002; Cagnoli 2003; Asteriou 2012). The test conditions of these studies are provided in Table 2 in comparison with our experiment. Our experiment differs from the other studies in terms of the size and mass of the samples. The other studies were limited to a

small scale to capture the block trajectory using a high-speed video camera. In our test, the high-speed video camera is replaced by a 3D motion capture system, which allows larger specimens to be considered.

Table 2. Test conditions of the previous studies versus our experiment

	Wang 2018	Chau 2002	Cagnoli 2003	Asteriou 2012
Sample shape	Spherical Polyhedron	Sphere	Cylinder	Cubic
Sample material	limestone	dental plaster	pumice	marble/sandstone/marl
Landing plate material	concrete	dental plaster	pumice	marble
Sizes (mm)	100/200	18.35/60/60	d=5.9,l-=8.5	20
Mass (g)	1200/10000	6.05/153.64/204.33	0.11	19.9/20.3/16.5
Impact velocities (m/s)	6.7-9.3	4-5.65	24.88	3
Impact angles	6°-60°	20°-80°	18°-74°	16°-77°
Roughness of the target surface	uneven	flat	flat	smooth
Sharpness of the specimens	rear edges	no edges	rear edges	smooth edges

Although the previous studies imposed various test conditions, they provided references for us to evaluate our results. Fig. 11 shows the effects of the impact angle on R_n, R_t and R_E provided by Chau (2002), Cagnoli (2003), Asteriou (2012) and our tests. In the absence of detailed data, only the trend line results in the literature are extracted and redrawn in Fig. 11 to make a comparison. In Chau's results, the specimen with a mass of 204.33 g was selected because that mass is closest to those of our samples. In Asteriou's results, we chose a marble specimen as the reference because marble and limestone have nearly the same hardness. As illustrated in Section 4.3, the rebound angle is typically less than the impact angle in the ideal state considering that energy dissipation occurs during the collision. Therefore, an additional trend line is added in Fig. 11 for our experiment after excluding those non-ideal data points that have a rebound angle larger than 1.2 times the impact angle. For the same reason as in Section 4.3, no differentiation between data of two sizes is made for our experiments here. Although results of the previous studies and our tests are quite different when they are plotted in one figure, some general trends could be observed.

Nat. Hazards Earth Syst. Sci. Discuss., https://doi.org/10.5194/nhess-2018-108
Manuscript under review for journal Nat. Hazards Earth Syst. Sci.
Discussion started: 24 April 2018

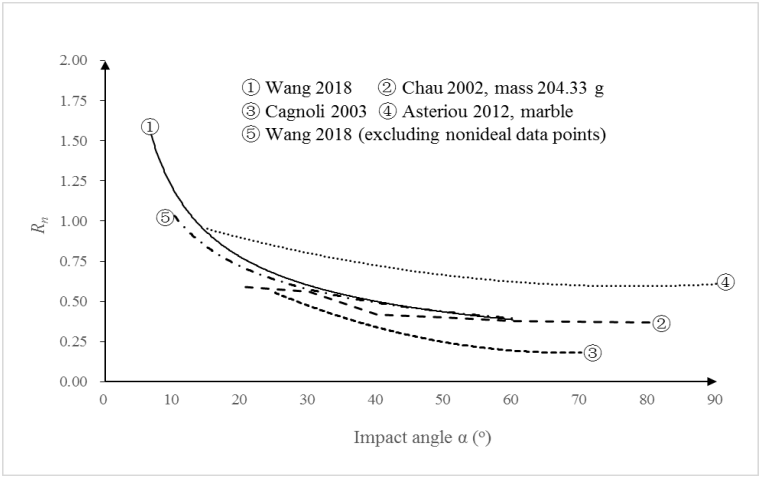

(a) R_n versus impact angle

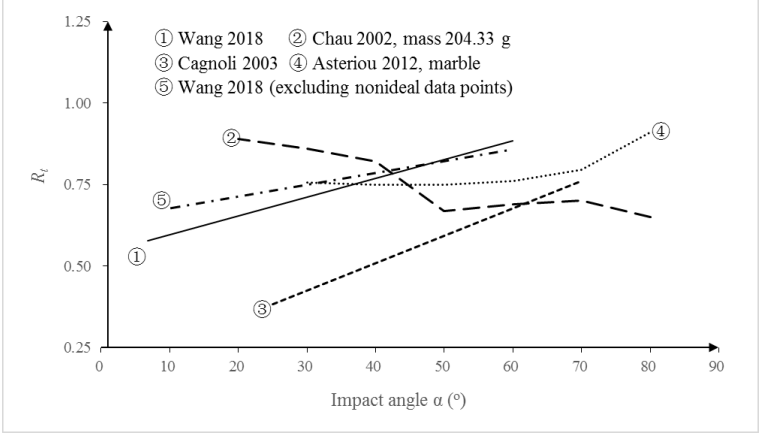

(b) R_t versus impact angle

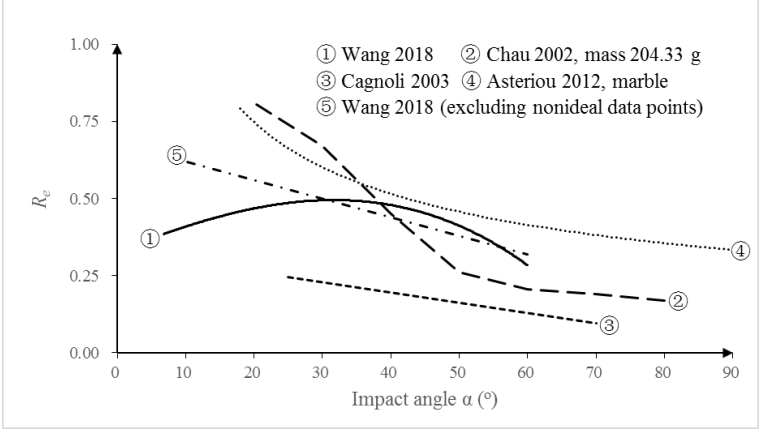

(c) R_E versus impact angle

Fig. 11. Comparison with other laboratory test results

Nat. Hazards Earth Syst. Sci. Discuss., https://doi.org/10.5194/nhess-2018-108
Manuscript under review for journal Nat. Hazards Earth Syst. Sci.
Discussion started: 24 April 2018

Natural Hazards and Earth System Sciences Discussions

First, all of the trends in R_n versus the impact angle are consistent, as shown in Fig. 11(a): R_n decreases with increases in the impact angle. Asteriou's tests offered the maximum R_n, which can be attributed to the lighter mass and lower impact velocities adopted in the tests. The minimum R_n occurred for the lightest specimens in Cagnoli's test, which may be due to the high impact velocity. The impact velocity of 24.88 m/s is sufficiently high to dissipate kinetic energy in additional forms, such as surface erosion and particle breakage. In Cagnoli's test, an indentation was observed upon impact. Compared to the other tests, our results produce the steepest descent in the beginning of the trend line. However, after excluding those non-ideal data points, the new trend of R_n versus the impact angle α is approximately linear. Several types of functions are used to match the new correlation of R_n versus the impact angle α in our tests, and results are listed below.

$$R_n = 1.0601e^{-0.018a}, R^2 = 0.7117 \quad (7\text{-}1)$$

$$R_n = -0.0099a + 0.9386, R^2 = 0.6977 \quad (7\text{-}2)$$

$$R_n = -0.307\mathrm{In}a + 1.6473, R^2 = 0.6578 \quad (7\text{-}3)$$

$$R_n = 3.6553a^{-0.544}, R^2 = 0.6334 \quad (7\text{-}4)$$

According to Eqs. (7-1)-(7-4), the correlation coefficient R^2 does not differ by a sufficiently large amount to determine the best fitting equation. Linear functions have been used to match the correlation of R_n and the impact angle α in several reports in the literature (Wu, 1985; Richards et al., 2001), although we cannot make a definitive conclusion that linear functions are the best choice in our study.

Next, Fig. 11(b) indicates that the changing trends of R_t versus the impact angle are rather scattered. Except for Cagnoli's result, the R_t obtained in the tests are all in the range from 0.5 to 1.0. Wu (1985) suggested that R_t may decrease slightly with increases in the slope angle θ. In other words, R_t may exhibit a small improvement with increases in the impact angle α. However, Chau's results contradicted Wu's suggestion. Even if those non-ideal data points obtained in our study are excluded, the new rising trend was trivial compared with the original trend. Various functions have considered to match the new trend, but the maximum correlation coefficient R^2 is less than 0.5 for all options considered. The new trend is still drawn as a linear correlation in Fig. 11(b). Considering the inconsistency of different test results and the small value of the correlation coefficient R^2 in our study, we cannot reach a definite conclusion regarding the effect of the impact angle α on R_t. Nonetheless, the impact velocity will influence the variation range of R_t. The nadir value of R_t decreases with increases in the impact velocity, which is a distinction between Cagnoli's result and the other results. Assuming that no larger difference in the impact velocity occurs between the two experiments, the variation range of R_t occurs regardless of the test conditions.

Finally, Fig. 11(c) shows the changing trends of R_E versus the impact angle. The other three experiments resulted in downward trend lines despite the different forms, which implies that increasing the impact angle will induce more energy dissipation. The trend line based on our results appears unreasonable considering the ascending curve in the beginning of the test. However, if those non-ideal data points are ignored, the new trend line is more comparable with the other trend lines. If the reserved data points are matched using a linear function, the result is

$$R_E = -0.0099a + 0.679, R^2 = 0.5815 \quad (8)$$

A comparison of Eq. (8) with Eq. (6) illustrates that the correlation coefficient R^2 is noticeably higher in Eq. (8), which indicates that the non-ideal data points hinder the correlation between the energy coefficient R_E and impact angle α. For different tests, the energy dissipation levels appear to be correlated with the normal coefficient R_n. Asteriou's test provided the maximum R_n and lowest energy dissipation level, whereas Cagnoli's provided the minimum R_n and highest energy dissipation level.

In conclusion, various experimental conditions produce various results for R_n, R_t and R_E, although there are certain trends that occur regardless of the test conditions. Both the normal coefficient of restitution R_n and the energy coefficient of restitution R_E decrease with increases in the impact angle. The tangential coefficient of restitution R_t is not affected by the impact angle. Our study did not provide strong evidence that the size and mass of blocks can affect the coefficients of restitution. The impact velocity is an important factor in appraising different tests because impact velocities with diverse levels in two tests may cause a remarkable difference in the resulting coefficients of restitution. If those data points with unexpected rebound angles are omitted, the modified trend lines are more comparable with the other trend lines, and the correlation between R_E and the impact angle α can be improved.

6 Discussion

The difference in changing trends between our results and the other experiments from the literature originates primarily from the non-ideal data points. As noted in Section 4.3, the phenomenon of a rebound angle that is larger than the impact angle always occurs when the impact angle is small. The probable reason and consequences of this trend are discussed in this section.

In our study, the landing plate was made of concrete slabs that have a smaller hardness value than the falling blocks. The impacts caused distinct damage on the surface, which can be attributed to the rear edges of the falling blocks. Provided that the indentation is caused by the impact, as shown as Fig. 12, the rebound angle is constrained by the configuration of the indentation if only parallel motion is involved. The restriction is less susceptible to the small rebound angle, because a parallel motion along the dashed red line indicates additional penetration. When the impact angle is sufficiently large to generate a rebound angle allowed by the restriction, the block may leave the surface with a parallel motion. However, in the case of a small impact angle, rotation motion must be involved to overcome the constraint. As Broili (1973) noted, the rotation moment generated from impact typically results in an increased normal velocity and reduced tangential velocity, and the rebound angle will be larger than the impact angle. Therefore, the penetration caused by the impact may contribute to the large rebound angle under small impact angles.

Furthermore, those damages on the surface constitute macro roughness, which also plays a role in generating larger rebound angles. Assume that the macro roughness of the landing plate is represented as a small inclined stair in Fig. 13; then, the interaction between the falling block and surface may have two stages in certain situations. The block impacts the surface before the stair and starts leaving in the first stage. Then, the block contacts the inclined stair and the velocity changes again

Nat. Hazards Earth Syst. Sci. Discuss., https://doi.org/10.5194/nhess-2018-108
Manuscript under review for journal Nat. Hazards Earth Syst. Sci.
Discussion started: 24 April 2018

in the second stage. The time interval between the two stages is sufficiently short that the two stages appear to finish simultaneously. Therefore, because the velocity changed by the stair is treated as the rebound velocity, the rebound angle is greater than the impact angle.

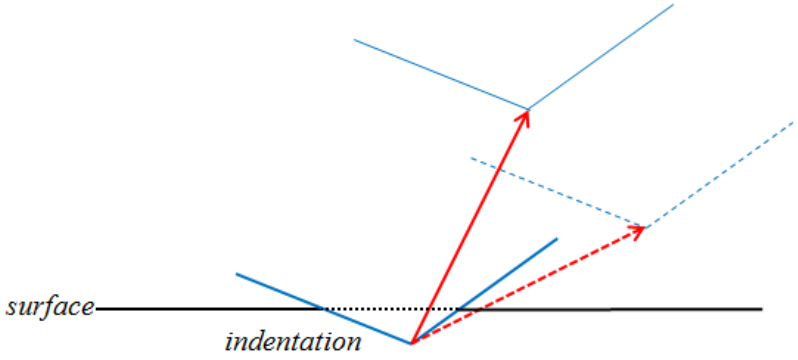

Fig. 12. Effect of indentation on the rebound angles

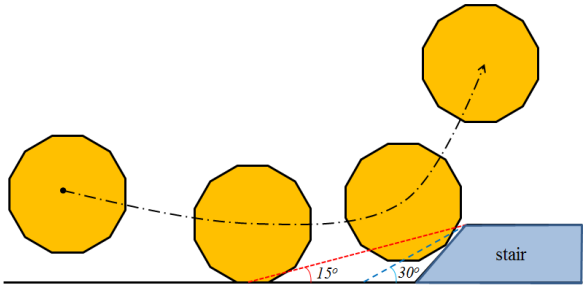

Fig. 13. Effect of macro roughness on the rebound angles

Given a fixed stair in Fig. 13, the impact angle determines whether the two-stage interaction occurs. Considering that a small impact angle will, in theory, induce a smaller rebound angle, it will increase the risk of the block contacting the stair when leaving the surface. As illustrated in Fig. 13, if the default rebound angle is 15°, the stair can affect the rebound behaviour when the block contacts the surface within 3.73 times the stair height before the stair. Therefore, the rebound angle will likely exceed the impact angle when the impact angle is small.

Of the various consequences of the rebound angle being greater than the impact angle, high values of the normal coefficient of restitution R_n may be most remarkable. Although engineers typically take unity as the upper bound of R_n in computer simulations, several scholars had reported R_n values greater than unity (Azzoni et al. 1992; Paronuzzi 2009; Spadari et al. 2012). Considering the basic definition in Section 2.1, we can obtain

$$R_n = \frac{v_{nr}}{v_{ni}} = \sqrt{R_E} sin\beta / sin\alpha \quad (9)$$

By introducing an angle coefficient

$$\lambda = sin\beta / sin\alpha \quad (10)$$

Nat. Hazards Earth Syst. Sci. Discuss., https://doi.org/10.5194/nhess-2018-108
Manuscript under review for journal Nat. Hazards Earth Syst. Sci.
Discussion started: 24 April 2018

Natural Hazards and Earth System Sciences
Discussions

Eq. (9) can be simplified as

$$R_n = R_E^{0.5}\lambda \tag{11}$$

Fig. 14 plots the relationship between R_n and the angle coefficient λ under different energy losses. The value of R_n increases when increasing the angle coefficient λ. Even if the coefficient of energy restitution R_E is only 0.3, R_n is greater than 1.0 when λ>1.83. An extremely large rebound angle is not needed to generate such an angle coefficient when the impact angle is small. For example, assume that the impact angle is 12° and 15°; then, a rebound angle of 22.4° and 28.3° is sufficient to obtain λ>1.83. Assuming that the degree of energy dissipation is unchanged, a case where the rebound angle is larger than the impact angle must lead to a higher R_n. Although the value of λ corresponding to R_n=1.0 varies with R_E, the condition λ>1.0 is required to obtain an R_n greater than unity. As shown in Fig. 14, R_n cannot exceed 1.0 if the rebound angle is lower than the impact angle.

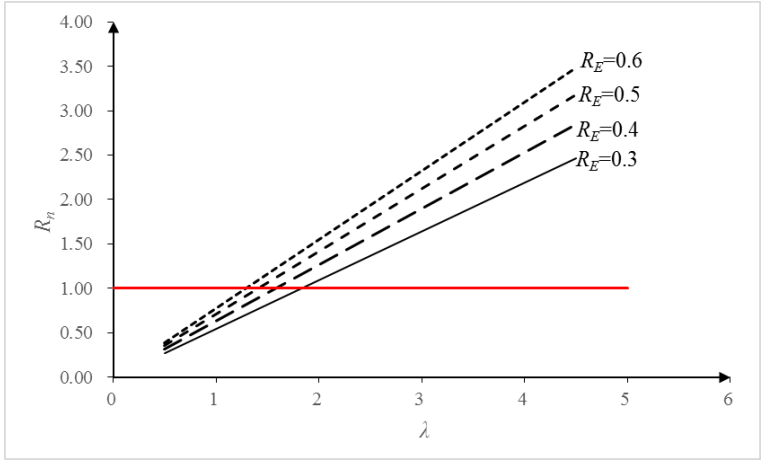

Fig. 14. R_n versus the angle coefficient λ

In conclusion, small impact angles may result in unexpected large rebound angles. If the angle coefficient λ formed by the rebound and the impact angle is sufficiently large, R_n will exceed unity even though R_E is small. Furthermore, assuming a constant energy dissipation level, the reduction in the impact angle decreases the threshold value of the rebound angle that should be satisfied to achieve an R_n in excess of unity, which means that smaller impact angles are more likely to yield a high R_n.

Then, it is unreasonable to simply treat a higher value of R_n as a symbol of lower energy dissipation. The normal restitution coefficient R_n has generally been associated with the degree of energy loss due to the elastic-plastic response of the surface material (Giani 1992). The results of our experiment demonstrate that given a small impact angle, the unexpected rebound angle generates a high R_n but causes more energy dissipation. The data for R_n and R_E are illustrated in Fig. 15. Increasing R_n will increase R_E initially but decrease it overall. The trend of R_E versus R_n is highly complex. For simplicity, two boundaries (R_n=0.65 and R_n=0.85) are added in Fig. 15. The coefficient of energy restitution R_E increases with increasing R_n when R_n<0.65, in agreement with the relationship between R_n and the energy loss level based on the elastic-plastic response

Nat. Hazards Earth Syst. Sci. Discuss., https://doi.org/10.5194/nhess-2018-108
Manuscript under review for journal Nat. Hazards Earth Syst. Sci.
Discussion started: 24 April 2018

analysis. If R_n is greater than 0.85, a larger R_n indicates a smaller R_E. High values of R_n are associated with unexpected rebound angles in our study, which means that the unexpected rebound angles can be related to higher energy dissipation. R_E is disordered if R_n lies in (0.65, 0.85), which is caused by the two different trends meeting. Therefore, the value of R_n could not be used to evaluate the energy dissipation level directly.

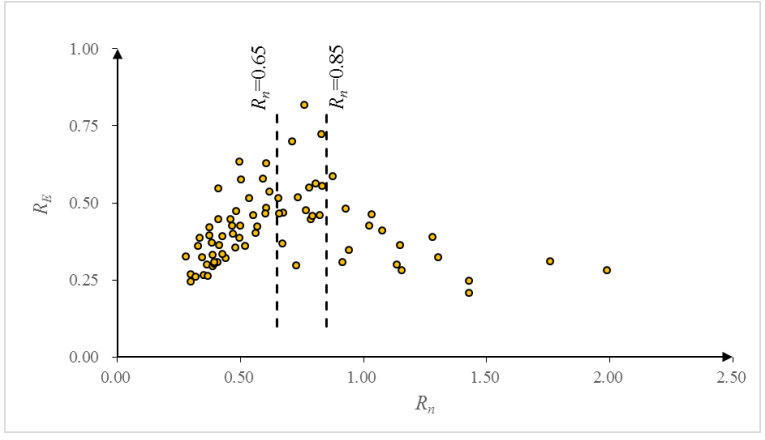

Fig. 15. R_E versus R_n

7 Conclusions

The coefficients of restitution are critical parameters predicting rockfall trajectory by computer simulations, while their values vary with the impact conditions. Both the terrain characteristics and kinematic parameters can significantly influence the variations in the restitution coefficients. The correlation between the impact angles and coefficients of restitution have been observed and investigated in a series of tests. Existing laboratory experiments have largely been limited to a small scale, and the scalability of results is uncertain.

In the present study, laboratory tests were performed using a 3D motion capture system. Spherical limestone polyhedra with diameters of 10 cm and 20 cm were taken as samples, and C25 concrete slabs were adopted to form the landing plate. By altering the release height and the inclined angle of the landing plate, the effects of the impact angle on the coefficients of restitution were estimated under freefall test conditions. The results verify the strong correlation between the normal coefficient of restitution R_n and the impact angle α. Regardless of the test conditions, several general laws occur when accounting for the effect of the impact angle. Both R_n and the energy coefficient of restitution R_E will decrease with increases in the impact angle. The upward trend of the tangential coefficient of restitution R_t versus the impact angle is negligible when considering its variation range. Compared to the sample size and mass, the impact velocity should be further considered when comparing different tests.

When the impact angle is less than 30°, the rebound angle may exceed the impact angle. The potential is increased with further decreases in the impact angle, leading to a higher R_n and lower R_E, which disturbs the regularity regarding the effect

of the impact angle and causes extreme scatter in the measured data, inducing more trouble in rockfall simulations using the normal and tangential coefficients of restitution. If the impact angle is small, the variation range of the coefficient of restitution is large, particularly for R_n, which means that using the representative value in the simulation is unreliable. The stochastic model may be more appropriate for analysing rockfall hazard (Jaboyedoff et.al, 2005; Frattini et.al, 2008; Bourrier et.al, 2009;) because it can account for the variation of the restitution coefficient based on data collection. Therefore, efforts should be made to obtain a comprehensive understanding of the variations in the coefficients of restitution with the kinematic parameters and terrain characteristics. A database of the coefficients of restitution from various experiments should be established to develop more robust stochastic rebound algorithms.

Acknowledgements

The study is supported by the Open Research Programme of the Hubei Key Laboratory of Disaster Prevention and Mitigation (under Grant No. 2017KJZ03) and the National Natural Science Funds (Project No. 51409150).

References

Agliardi F, Crosta GB (2003) High resolution three-dimensional numerical modelling of rockfalls. International Journal of Rock Mechanics and Mining Sciences 40, 455–471.

Asteriou P, Saroglou H, Tsiambaos G (2012) Geotechnical and kinematic parameters affecting the coefficients of restitution for rock fall analysis. Int J Rock Mech Min Sci 54:103-113

Azzoni A, Drigo E, Giani G, Rossi P, Zaninetti A (1992) In situ observation of rockfall analysis. In: Proceedings of the 6th international symposium on landslides, Christchurch, pp 307–314

Azzoni A, Barbera GL, Zaninetti A (1995) Analysis and prediction of rockfalls using a mathematical model. *International Journal of Rock Mechanics and Mining Science* 32, 709–24.

Bourrier F, Dorren L, Nicot F, Berger F, Darve F (2009) Toward objective rockfall trajectory simulation using a stochastic impact model, Geomorphology,110:68-79

Bozzolo D, Pamini R (1986) Simulation of rock falls down a valley side. Acta Mech 63:113–30.

Broili L (1973) In situ tests for the study of rockfall. Geol Appl Idrogeol, 8: 105–11

Buzzi O, Giacomini A, Spadari M (2012) Laboratory investigation on high values of restitution coefficients. Rock Mech Rock Eng 45:35–43

Cagnoli B, Manga M (2003) Pumice-pumice collisions and the effect of the impact angle. Geophysical Research Letters 30, 12:1636

Chau KT, Wong RHC, Wu JJ (2002) Coefficient of restitution and rotational motions of rockfall impacts. Int J Rock Mech Min Sci 39:69–77

Chau KT, Wong RHC, Liu J, Wu JJ, Lee CF (1999) Shape effects on the coefficient of restitution during rockfall impacts. Ninth International Congress on Rock Mechanics, ISRM Congress, Paris, p. 541–44.

Dorren LKA (2003) A review of rockfall mechanics and modelling approaches. Progress in Physical Geography 27 (1), 69–87.

Dorren LKA, Berger F, Putters US (2006) Real-size experiments and 3-D simulation of rockfall

Fornaro M, Peila D, Nebbia M (1990) Block falls on rock slopes-application of a numerical simulation program to some real cases. In: Proceedings of the 6th international IAEG congress, 2173-80

Frattini P, Crosta GB, Carrara A, Agliardi F (2008) Assessment of rockfall susceptibility by integrating statistical and physically-based approaches. Geomorphology, 94 (3-4), 419-437

Giani GP (1992) Rock Slope Stability Analysis. Rotterdam: Balkema

Giani GP, Giacomini A, Migliazza M, Segalini A (2004) Experimental and theoretical studies to improve rock fall analysis and protection work design. Rock Mech Rock Eng, 37(5):369–89.

Guzzetti F, Crosta G, Detti R, Agliardi F (2002) STONE: a computer program for the three dimensional simulation of rock-falls. Computer & Geosciences 28, 1079–1093.

Guzzetti F, Reichenbach P, Wieczorek GF (2003) Rockfall hazard and risk assessment in the Yosemite Valley, California, USA, Natural Hazards and Earth System Sciences, 3, 6:491-503

Habib P (1976) Notes sur le rebondissement des blocs rocheux. Meeting on Rockfall Dynamics and Protective Works Effectiveness, p. 20–1.

He SM, Wu Y, Yang XL (2008) Study of rock motion on slope. Chinese Journal of rock mechanics and engineering, 27(s1):2793-2798

Heidenreich B (2004) Small- and half-scale experimental studies of rockfall impacts on sandy slopes. PhD Thesis, Ecole Polytechnique Fédérale de Lausanne, Swiss.

Jaboyedoff M, Dudt JP, Labiouse V (2005) An attempt to refine rockfall zoning based on kinetic energy, frequency and fragmentation degree. Natural Hazards and Earth System Sciences, 5, 621–632

Jones C, Higgins JD, Andrew RD (2000) Colorado Rockfall Simulation Program User's Manual for Version 4.0. Denver: Colorado Department of Transportation

Pappalardo G, Mineo S, Rapisarda F (2014) Rockfall hazard assessment along a road on the Peloritani Mountains (northeastern Sicily, Italy), Natural Hazards and Earth System Sciences, 14, 10:2735-2748

Paronuzzi P (1989) Probabilistic approach for design optimization of rockfall protective barriers. Quart J Eng Geol, 22:175–83.

Paronuzzi P (2009) Field evidence and kinematical back analysis of block rebounds: the Lavone rockfall, Northern Italy. Rock Mech Rock Eng 42:783–813

Richards LR, Peng B, Bell DH (2001) Laboratory and field evaluation of the normal coefficient of restitution for rocks. In: Proceedings of Eurock pp. 149–56.

Robotham ME, Wang H, Walton G (1995) Assessment of risk from rockfall from active and abandoned quarry slopes. Trans Inst Min Metall A 104(1–4):A25–33.

Spadari M, Giacomini A, Buzzi O, Fityus S, Giani G (2012) In situ rock fall tests in New South Wales, Australia. Int J Rock Mech Min Sci 49:84-93

Scioldo G (2006) User guide ISOMAP & ROTOMAP-3D surface modelling and rockfall analysis. Geo&Soft International.

Stevens W. (1998) RockFall: a tool for probabilistic analysis, design of remedial measures and prediction of rock falls. MaSc thesis, University of Toronto

Wu SS (1985) Rockfall evaluation by computer simulation. Transp Res Rec 1031:1–5.